Nonlinear dynamic simulation of cable based structures interacting with sliding objects using the concept of macro element

David Bertrand, Stéphane Grange, Franck Bourrier, Thomas Langlade

Nonlinear dynamic simulation of cable based structures interacting with sliding objects using the concept of *macro element*.

D. Bertrand*, S. Grange, F. Bourrier and T. Langlade

December 14, 2020

Abstract

This paper presents the formulation of a finite element enclosing a specific internal mechanical equilibrium in order to model cable-based structures in dynamics conditions. It is based on the concept of *macro finite element* which allows embedding complex mechanical systems solved inside the element boundaries. A significant advantage is to allow an easy implementation within classical commercial codes. The proposed *macro finite element* describes a cable interacting with a sliding object assimilated to a punctual mass where friction can be accounted for. The dynamic response is described by a model developed within the framework of the DEM (Discrete Element Method) where geometrical nonlinearity (large displacements) is considered. A model combining the proposed macro finite element and a classical linear truss finite element is presented in order to validate its implementation. Finally, illustrative examples are presented. First, a cable yarning system is considered. The effect of friction and of the bending stiffness of the posts on the overall kinematics and force within the system are explored. Then the vulnerability of a cable-stayed bridge to earthquake is explored accounting for guy ropes failure.

Highlights

*Corresponding author : D. Bertrand, david.bertrand@insa-lyon.fr, tel : +33(4) 72 43 72 94, fax : +33 (0)4 72 43 85 21

- Macro finite element implementation and validation. Combination of FEM and DEM
- Cable and sliding mass under large displacement connected to beam finite elements
- Validation and application on cable based structures in dynamic conditions

1 Introduction

During the last decades, the cable-based structures have been widely used in many fields and especially for civil engineering purposes (cable stayed bridges [AAG95], [ZC14], [FS11], rockfall protections [DBYK11], [GGM+12], [MGB+16], tensegrity structures [BB04], cable yarning operations [DBB16]). The modelling of such structure is always a challenge because of the significant geometrical nonlinear behaviour that can develop in particular when dynamic loadings are considered. Moreover, the sliding between structural components (cable/beam, cable/cable, *etc.*) is of first importance for application problems such as tensegrity structures or cable anchored protection structures. For instance, in order to describe correctly the evolution of the shape of a rockfall protection during an impact, the sliding of each cable on the other ones should be accounted for to get a good assessment of the force distribution within the structure ([Alb16], [CCLN17], [DCB+19]). Because they are very deformable, the force distribution is very sensitive to the shape these structures will take during the impact interaction.

Cable finite element formulations are generally mathematically cumbersome and rarely universal. Many continuous models of cable have been proposed ([Irv81], [DV99], [TK11]). Most of the approaches are based on either analytical resolution (catenary theory) or numerical simulation, often carried out with the finite element method. In the latter case, the formulation of the cable finite elements (*inter alias* the derivation of the stiffness matrix) are not straightforward and can expose to difficulties from a mathematical point of view. For instance, [WC89] proposed a cable finite element formulation in dynamic conditions accounting for large deflection and based on elastic material. A moving mass is considered but the latter is treated as an external load with no reciprocal interaction between the cable and the moving object. Within this paper, the macro finite element formulation is much simpler (no stiffness matrix derivation) and the moving load (the sliding mass) is considered as a system by itself. [Auf93] proposed also a cable finite element, which is able to pass through a pulley, but based on restrictive assumptions. Indeed, the pulley cannot reach the extremities of the cable and the pulley stays between the nodes of the cable element (no possible passage between cable elements). From an algorithmic point of view, the update of the mass matrix should be performed at each timestep and [Auf93] related problems of convergence of Newton-Raphson algorithm because of the finite element singularity of the stiffness matrix. [TIWYM94] proposed

to model cable interaction with "riding" accelerating mass based on Fourier series decomposition with the superimposition of the dynamic solution over the static solution ([AQNO03] proposed the same kind of approach based on Fourier series and wavelet formulations without friction). They suppose that the cable is inextensible and they account for the friction between the sliding mass and the cable. Although relevant, [TIWYM94]'s method is less flexible/adaptable compared to classical FEM and DEM approaches. [JC05] formulated in static conditions, a super element (accounting for multiple pulleys) which can describe material and geometrical nonlinearity and also friction effects. The main limitation is that only static case can be considered.

Alternatively to the finite element method, cable systems have been modelled within the framework of the discrete element method ([NCM01], [BTLS12]). This method is particularly well adapted to account easily for the potential nonlinearity onset (geometrical and material) under static or dynamic conditions. The main interest to use DEM alternatively to FEM for cable modeling, is an easy resolution process, without any constraining assumptions about the kinematics of the rope and the sliding mass(es). Thus, the case of moving load/object along the cable can also be considered in a simple way. [CCLN17] proposed within the DEM framework to model cable based structures where dynamic, material and geometrical nonlinearities are accounted for. They also describe the relative movement of cables linked by pulleys. This advanced cable modeling is very efficient but within the framework of DEM, can lead to prohibitive computational costs. In addition, describing continuous structures (such as beam, plate, *etc.*) is not straightforward within the DEM framework.

To solve such problems involving cable based elements, the proposed *macro finite element* formulation is particularly interesting. The main advantage of the proposed approach is to take advantage of the both DEM and FEM in terms of flexibility and easiness of implementation. From a practical point of view, once the macro finite element is formulated, it can be used as a new finite element in any sort of finite element codes. The complexity related to the mechanical system is integrated within the macro finite element (specific internal kinematics) and the overall finite element resolution process is not modified.

In this paper, the macro finite element proposed embeds the dynamic response of a sliding mass and a cable. The discrete element method (DEM) is chosen to model the cable and the sliding mass kinematics with the help of an explicit integration scheme. The communication between the macro

finite element and the rest of the finite elements is performed *via* the nodal displacements and nodal forces, without the need to compute anything else from the macro finite element (no tangent matrix computation). A particular attention should be paid to consider the same integration scheme at the overall code scale and within the macro finite element ([CG02]). Thus, the motion equations are solved with an explicit integration scheme in the finite element code (explicit central differences based on predictor-corrector integration rule). Complex mechanical systems composed of drastically different parts (such as cables and rigid posts) that involves antagonist assumptions (small/large strains/displacements, impact interaction, different numerical methods, *etc.*) can be mixed easily.

In the next sections, the discrete element models used to simulate the dynamic sliding of an object onto a cable are described. Then, their implementation within a macro finite element is presented. Next, two examples are discussed which concern the simulation of a cable yarning system and a cable-stayed bridge.

2 Material and Methods

2.1 Discrete modelling of an elastic cable

The cable discrete model is based on [Wil06]'s approach. It is assumed that the cable is perfectly flexible (no bending moment, only pure traction can appear within the cable). For the sake of simplicity, the mechanical behaviour of the cable is supposed linear elastic but its behaviour can be easily extended to non linear constitutive laws. The model is discretized into elements (Figure 1a) delimited by nodes which are evenly spaced along the cable curvilinear abscissa. Each node carries a mass calculated from the total mass of the cable.

The inputs parameters are the cable initial length (L_c^{ini}), the diameter of the cable cross section ($d_c = 2r_c$), the cable *Young*'s modulus (E_c) and the cable density (ρ_c). The total mass of the cable (m_c) is distributed over each cable node and thus a node (i) has a mass of $m_i = m_c/(n_{CE}+1)$ where n_{CE} is the number of cable elements. The cable elements (resp. nodes) are labelled from 1 to n_{CE} (resp. from 1 to $n_{CE}+1$). The first node ($i = 1$) and the last node ($i = n_{CE}+1$) are the ends of the cable. The cable discretization is uniform and the initial length of a cable element is $l_{ini} = L_c^{ini}/(n_{CE}+1)$.

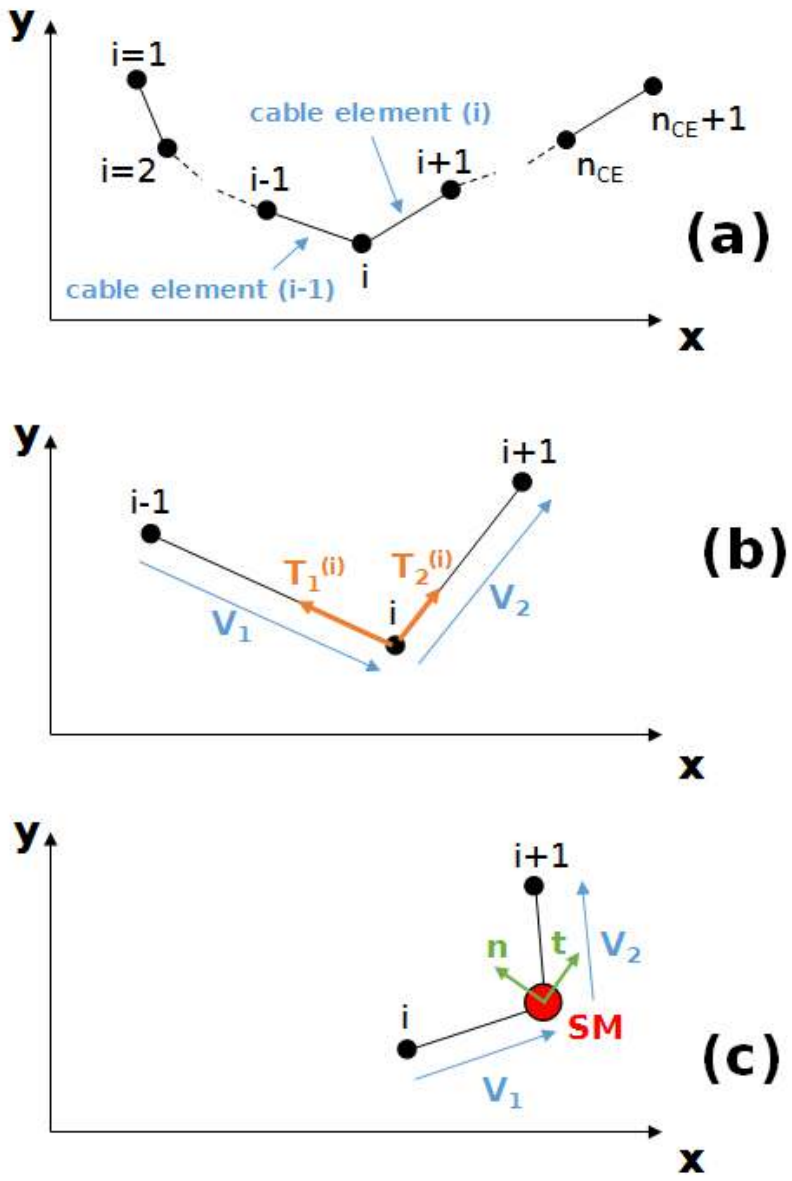

Figure 1: Discrete model of the cable and numbering of the cable nodes (black dots) and cable elements (black lines). Cable meshing (without sliding mass) into cable elements (black lines) and nodes (black dots) (a), tension forces ($\vec{T_1}^{(i)}$ and $\vec{T_2}^{(i)}$) applied on the i^{th} cable's node (i) due to the neighbouring nodes ($i-1$ and $i+1$)(b). Accounting for a sliding mass (in red), here belonging to the cable element, between nodes i and $i+1$ (c).

In addition to external loadings (such as gravity), each node interacts with its neighbouring nodes (Figure 1b). For a node i, the tension forces ($T_1^{(i)}$ and $T_2^{(i)}$) are calculated from

$$\vec{T_1^{(i)}} = E_c A_c \epsilon^{(i-1)} \vec{n_1} \quad \text{with} \quad \vec{n_1} = \frac{-\vec{V_1}}{\|\vec{V_1}\|} \tag{1}$$

$$\vec{T_2^{(i)}} = E_c A_c \epsilon^{(i)} \vec{n_2} \quad \text{with} \quad \vec{n_2} = \frac{\vec{V_2}}{\|\vec{V_2}\|} \tag{2}$$

where $\vec{V_1}$ (resp. $\vec{V_2}$) is the branch vector from nodes $i-1$ to i (resp. i to $i+1$) when no sliding mass is considered (Figure 1b). A_c is the cable effective cross section area. Axial strains of the cable elements ($\epsilon^{(i-1)}$ and $\epsilon^{(i)}$) can be expressed from the initial ($l_{ini}^{(i-1)}$ and $l_{ini}^{(i)}$) and current ($l^{(i-1)}$ and $l^{(i)}$) lengths as

$$\epsilon^{(i)} = \frac{l^{(i)} - l_{ini}^{(i)}}{l_{ini}^{(i)}} \tag{3}$$

For each node (i), the second *Newton*'s law leads to

$$m_i \vec{\ddot{u}}^{(i)} = m_i \vec{g} + \vec{T_1}^{(i)} + \vec{T_2}^{(i)} \tag{4}$$

where $\vec{\ddot{u}}^{(i)}$ is the second time derivative of the node displacement ($\vec{u}^{(i)}$) and $\vec{g}$ is the gravity acceleration.

The dynamic problem is solved through time with an explicit numerical integration scheme based on central finite difference where a predictor-correction step is used.

2.2 Sliding object onto an elastic cable

Accounting for a sliding object (so-called the sliding mass (**SM**) in the following) onto a cable does not change the preceding resolution process. The main point is to assess the forces coming from the sliding object to the cable during the motion of the mass (and *vice et versa*). First, the mechanical balance is carried out on a single cable element. The action of the sliding mass onto the cable element is exposed without friction and then accounting for friction. Then, the generalisation to multiple cable elements is described.

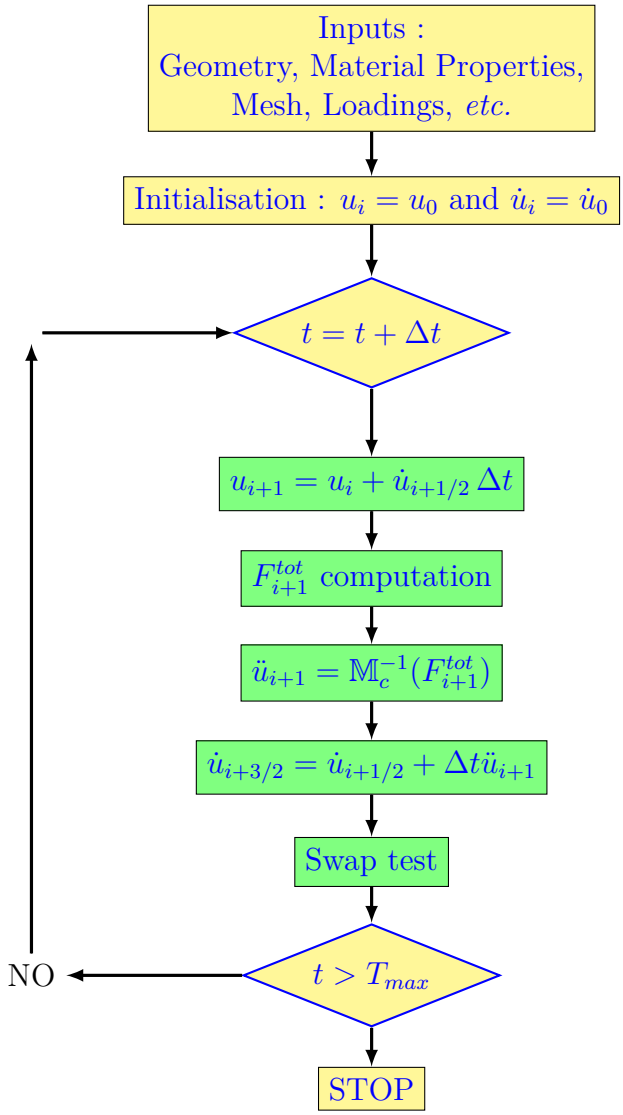

Figure 2: Resolution algorithm of a cable interacting with a sliding mass based on explicit integration scheme. The simulation time is T_{max}. The following notation is adopted: $t_i = i\Delta t$ and $x_i = x(t_i)$ where x can be either displacements, velocity or accelerations of the cable nodes. $\mathbb{M}_c$ is the mass matrix of the cable elements composing the cable, F^{tot}_{i+1} is the force balance applied on each cable node computed form the cable node displacements u_{i+1}. The swap test is only active when a sliding mass is considered and interacts with the cable (Figure 3).

2.2.1 Case of a single cable element

At given time t, the sliding mass is supposed in between the two cable nodes i and $i+1$ (Figure 1c). The center of mass of the sliding object can be considered as a moving node that belongs to the cable, interacting with the other cable nodes. The problem consists in solving the dynamic equation for the sliding mass onto a single cable element. If the friction is neglected, the equation of motion of the sliding mass can be written as

$$m_{\mathbf{SM}}\ddot{\vec{u}}_{\mathbf{SM}} = m_{\mathbf{SM}}\vec{g} + \vec{F_s^N} \tag{5}$$

where $m_{\mathbf{SM}}$ is the mass of the sliding object and $\vec{u}_{\mathbf{SM}}$ its displacement, $\vec{F_s^N}$ is the cable force acting on the sliding mass. In order to compute those forces, a Cartesian coordinate system is defined, composed of unit vectors ($\vec{n}$, $\vec{t}$ and $\vec{k_n}$). $\vec{k_n}$ is the orthogonal vector to the plane defined by the two nodes (i and $i+1$) and the sliding mass (Figure 1c). $\vec{n}$ belongs to the previous plan and is along the bisector of vectors $\vec{V_1}$ and $\vec{V_2}$. Note that the definition of $\vec{V_1}$ and $\vec{V_2}$ is modified due to the presence of the sliding object on the cable element i. $\vec{t}$ is the vector completing the direct triad. Their expressions are

$$\begin{cases} \vec{k}_n = \dfrac{\vec{V_1} \wedge \vec{V_2}}{\|\vec{V_1} \wedge \vec{V_2}\|} \\ \vec{n} = \dfrac{1}{2}\left(\dfrac{\vec{V_1} \wedge \vec{k}_n}{\|\vec{V_1} \wedge \vec{k}_n\|} + \dfrac{\vec{V_2} \wedge \vec{k}_n}{\|\vec{V_2} \wedge \vec{k}_n\|}\right) \\ \vec{t} = \vec{k}_n \wedge \vec{n} \end{cases} \tag{6}$$

Because no friction is accounted for, and due to the *Capstan* equation, cable tensions ($\|\vec{T_1}\|$ and $\|\vec{T_2}\|$) on each sides of the sliding mass are equal in terms of magnitude. It involves that the direction of the resultant force of the cable applied on the sliding mass is along $\vec{n}$.

$$\vec{F_s^N} = (\vec{T_1} \cdot \vec{n} + \vec{T_2} \cdot \vec{n})\vec{n} \tag{7}$$

Moreover, $\vec{T_1}$ and $\vec{T_2}$ can be expressed such as

$$\vec{T_1} = -T\frac{\vec{V_1}}{\|\vec{V_1}\|} \quad \text{and} \quad \vec{T_2} = T\frac{\vec{V_2}}{\|\vec{V_2}\|} \tag{8}$$

Because the cable is supposed elastic and only one cable element is considered (*i.e.* $L_c^{ini} = l_{ini}$), the tension reads

$$T = \|\vec{T_1}\| = \|\vec{T_2}\| = \frac{E_c A_c}{l_{ini}}(\|\vec{V_1}\| + \|\vec{V_2}\| - l_{ini}) \tag{9}$$

The extension to the case with friction leads to suppose that an additional force appears along $\vec{t}$. The latter is assessed based on the *Coulomb*'s friction theory. Within the equation of motion of the sliding mass, a tangential force ($\vec{F_s^f}$) is now considered. The equation of motion takes the form

$$m_{\mathbf{SM}}\ddot{\vec{u}}_{\mathbf{SM}} = m_{\mathbf{SM}}\vec{g} + \vec{F_s^N} + \vec{F_s^f} \tag{10}$$

The sum of the external forces $\vec{F}_{ext}$ (here only $m_{\mathbf{SM}}\vec{g}$) acting on the sliding mass are computed. *Coulomb*'s law implies that the maximum friction force is limited to $F_{max}^f = \mu\|\vec{F_s^N}\|$ where μ is the *Coulomb*'s friction coefficient. Thus, the friction force is defined as

$$\vec{F_s^f} = \begin{cases} -sign(\vec{V_R}\cdot\vec{t})\, F_{max}^f\, \vec{t} & \text{if} \quad |\vec{F}_{ext}\cdot\vec{t}| \geq F_{max}^f \\ -sign(\vec{V_R}\cdot\vec{t})|\vec{F}_{ext}\cdot\vec{t}|\,\vec{t} & \text{if} \quad |\vec{F}_{ext}\cdot\vec{t}| < F_{max}^f \end{cases} \tag{11}$$

where $\vec{V_R}\cdot\vec{t}$ is the relative velocity along $\vec{t}$ of the sliding mass with respect to the cable. The relative velocity is defined as $\vec{V_R} = \dot{\vec{u}}_{\mathbf{SM}} - \dot{\vec{u}}_{interp}$ where $\dot{\vec{u}}_{interp}$ is the linear interpolation of the cable velocity such as $\dot{\vec{u}}_{interp} = \frac{1}{\|\vec{V_1}\|+\|\vec{V_2}\|}(\|\vec{V_2}\|\dot{\vec{u}}_i + \|\vec{V_1}\|\dot{\vec{u}}_{i+1})$. When the frictional force is taken into account, the effect of friction forces needs to be transferred to the adjacent nodes (i and $i+1$) of the cable element (i). These forces modify the tension forces by adding the following terms on node (i) and ($i+1$)

$$\vec{F_i^f} = -\frac{\|\vec{V_2}\|\vec{F_s^f}}{\|\vec{V_1}\| + \|\vec{V_2}\|} \quad \text{and} \quad \vec{F_{i+1}^f} = -\frac{\|\vec{V_1}\|\vec{F_s^f}}{\|\vec{V_1}\| + \|\vec{V_2}\|} \tag{12}$$

Note that [Wil06]'s cable model may have modelling limitations related to the way the friction forces are calculated. When the cable angle is close to 90^o and when the cable discretization is not finer enough, unrealistic bending forces on the cable can exist. It is linked to the assumption that the pulley is a point and not a finite cylinder. To overcome this problem, several studies have been proposed (see for instance [LCJ03], [JC05]).

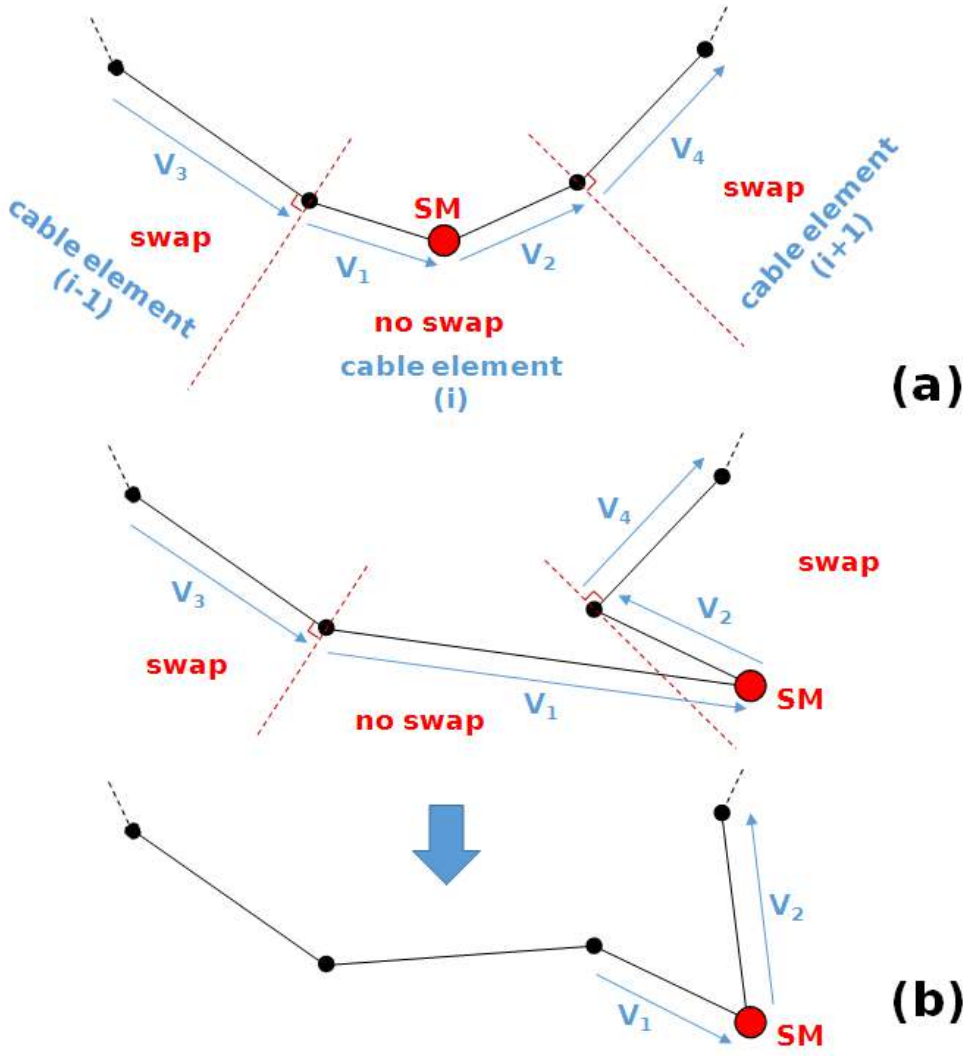

Figure 3: Swap procedure and passage condition of the sliding mass from a cable element to another one. No swap (a) : Passage condition not activated from the current cable element to the next one. Swap occurrence (b): Passage condition activated from the current cable element to the next one and associated remeshing.

2.2.2 Case of multiple cable elements

In order to get a fine description of the cable kinematics through time, the cable spatial discretization should involve several cable elements. Figure 2 depicts the flow chart for the resolution of the multi cable element system. First, at each time t, the cable element interacting with the sliding object should be identified as a function of its location along the cable curvilinear axis. Second, cable tensions on both sides of the sliding mass should be updated to account for its effect on the cable. A specific procedure has been developed to move the sliding mass from one cable element to another one, the so-called "swap procedure" in the following. The swap procedure algorithm is presented in figure 3. From a given time t, the criterion for swapping is based on bisector planes allowing to know if the swap should be activated or not as a function of the sliding mass position. It is also supposed that, if the sliding mass is on the first or the last cable element, the sliding mass cannot leave the cable. That being said, it is possible to let the sliding object go out the cable if wanted. At each timestep, vectors $\vec{V}_i$ (for $i \in \{1, 2, 3, 4\}$) are updated and the activation of the passing condition from a cable element to another one is written as

1. If sliding mass not on the first cable element ($i \neq 1$) and if $-\vec{V}_3 \cdot \vec{V}_1 > 0$ $\rightarrow$ sliding mass is swapped onto previous cable element ($i - 1$)

2. If sliding mass not on the last cable element ($i \neq n_{EC} + 1$) and if $-\vec{V}_4 \cdot \vec{V}_2 > 0 \rightarrow$ sliding mass is swapped onto the next element ($i + 1$)

2.3 *Macro finite element* implementation

The preceding cable and sliding mass model is implemented within a finite element code. The previous model is seen by the code as a finite element but having specific embedded features that describes the cable-sliding mass mechanical behaviour. The nodes of the macro finite element are the ends of the cable (cable nodes $i = 1$ and $i = n_{CE} + 1$). Thus, the macro finite element has only two nodes. Only the ends of the cable interact with the finite element code. Obviously, the presented case can be extended for instance by considering the sliding mass as a node too and allowing to extend the potential application fields. For a given time t, knowing the nodal displacements imposed at the cable ends ($U_{i+1}^{MacroFE}$), coming from the surrounding finite elements (here truss and *Timoshenko* beams, see next sections), it is

possible to proceed to the internal computation of the dynamic response of the cable-sliding mass system over a timestep (explicit integration scheme used within the macro finite element) where geometrical nonlinearities (large displacements) are treated. Then, for the next timestep, the nodal forces of the macro finite element ($F_{i+1}^{MacroFE}$) are returned to the nodes and applied on the surrounding finite elements. In order to be consistent with the calculation of the cable motion performed within the macro finite element, the same numerical integration scheme has to be used in the finite element code. Thus, the same explicit integration scheme (central finite differences based on predictor-corrector integration rule), and obviously the same timestep (dt), are used to calculate the kinematics variables (displacement U_i, velocity $\dot{U}_i$ and acceleration $\ddot{U}_i$) for each timestep. The general resolution process used is summarized in figure 4.

This approach takes advantages of both methods (FEM and DEM). Finite element simulations are particularly well suited to model continuous mechanical systems (for instance posts, beams, plates) where material can be treated with the help of nonlinear approaches. On the other hand, discrete element simulations are more adapted for simulation of discrete systems (cohesive or non cohesive granular matter, soil erosion, *etc.*) where contacts, cracks or large displacements can be treated in an easier way. In the present approach, the large displacements of the cable and the sliding mass are easily implemented. Furthermore, the extension to material nonlinearity is particularly straightforward within the DEM framework. The main limitation is the mandatory use of explicit integration schemes which are conditionally stable.

3 Validation under dynamic conditions

First, the validation of the cable-sliding mass model is performed by comparing the solution to a simple case taken from the literature for which an analytical solution of the problem has been proposed by [ZAL04]. Second, the macro finite element formulation and its implementation into a finite element code are validated considering the interaction between the macro finite element with a truss finite element. In order to explore both configurations, a validation model is considered which allows testing either the cable-sliding mass alone or the implementation of the macro finite element within a finite element code. The previous problem can be solved with alternative resolu-

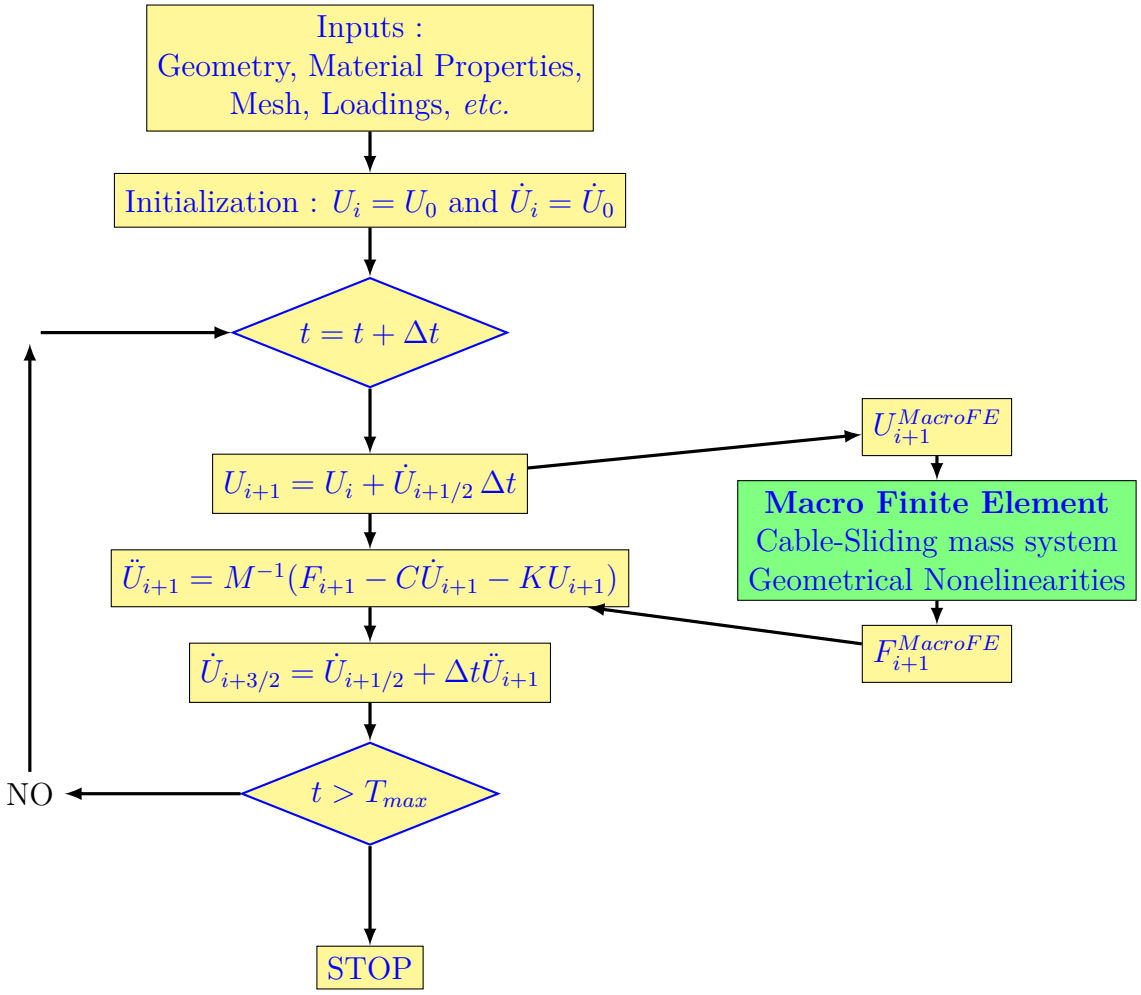

Figure 4: General resolution algorithm for a simulation time T_{max}. The following notations are adopted: $t_i = i\Delta t$ and $X_i = X(t_i)$ where X can be either displacements, velocities or accelerations.

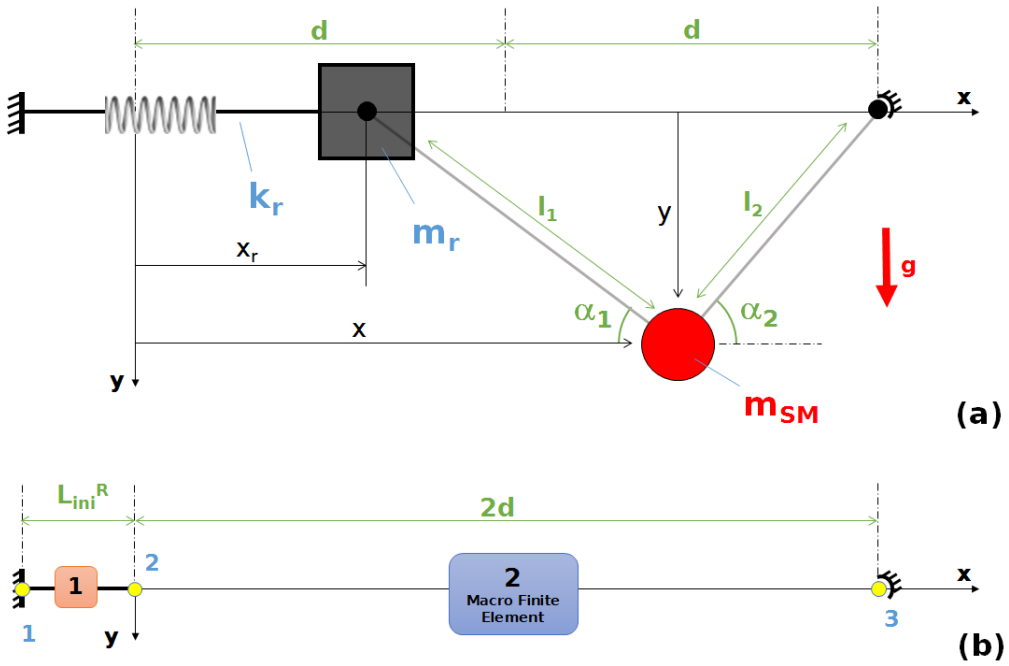

Figure 5: (a) Scheme of the validation model. A macro finite element (cable and sliding mass) connected to a truss element assimilated to a mass-spring system. (b) Finite element mesh. L_{ini}^R corresponds to the initial length of the spring when the spring is at rest ($x_r = 0$). The yellow circles correspond to the nodes of the mesh and the two finite elements of the mesh are symbolized by rectangles.

tion process based on *Runge-Kutta* solver (so-called in the following the `RK4` approach) which can serve to produce reference solutions.

3.1 Validation model

An elastic cable is considered where a sliding mass can move onto it. Gravity is active. The right end of the cable cannot move and the other end is fixed to a truss element which can be assimilated to a mass-spring system (so-called hereafter **MS**). The stiffness of the spring is k_r and its mass m_r. The mass of the **MS** can only develop a motion along the x axis. All the inputs of the problem are depicted within figure 5a. Because the cable is supposed elastic,

its total length (L_c) can vary through time. For a given time t, the cable tension (T), which is constant along the curvilinear axis of the cable when friction is neglected, is related to the cable elongation ($\Delta L_c = L_c - L_c^{ini}$) through

$$T = k_c \, \Delta L_c \tag{13}$$

where $k_c = E_c A_c / L_c^{ini}$ is the cable axial stiffness. The geometrical constraints (Figure 5) lead to the following equations

$$l_1(t)^2 = (x - x_r)^2 + y^2 \tag{14}$$
$$l_2(t)^2 = (2d - x)^2 + y^2 \tag{15}$$
$$L_c(t) = l_1(t) + l_2(t) \tag{16}$$
$$\cos\alpha_1 = \frac{x - x_r}{l_1} \tag{17}$$
$$\cos\alpha_2 = \frac{2d - x}{l_2} \tag{18}$$
$$\sin\alpha_1 = \frac{y}{l_1} \tag{19}$$
$$\sin\alpha_2 = \frac{y}{l_2} \tag{20}$$

The overall deformation of the system is controlled by three parameters and the purpose is to find the time evolution of x, y and x_r, which are respectively the position of the sliding mass and the displacement of the mass connected to the spring. When friction is considered, an additional force ($\vec{F}_s^f$) is computed such as presented in the previous section.

The mechanical balance of the sliding mass is described in figure 6b and leads to the following equations

$$T\cos\alpha_2 - T\cos\alpha_1 + \vec{F}_s^f.\vec{x} = m_{\mathbf{SM}}\,\ddot{x} \tag{21}$$
$$m_{\mathbf{SM}}\,g - T\sin\alpha_2 - T\sin\alpha_1 + \vec{F}_s^f.\vec{y} = m_{\mathbf{SM}}\,\ddot{y} \tag{22}$$

where $T = k_c \, \Delta L_c$ is a function of x, y and x_r. It can be rewritten as

$$\Delta L_c = \Delta l_1 + \Delta l_2 \quad \text{with} \tag{23}$$
$$\Delta l_1 = l_1 - l_1^{ini} \tag{24}$$
$$\Delta l_2 = l_2 - l_2^{ini} \tag{25}$$

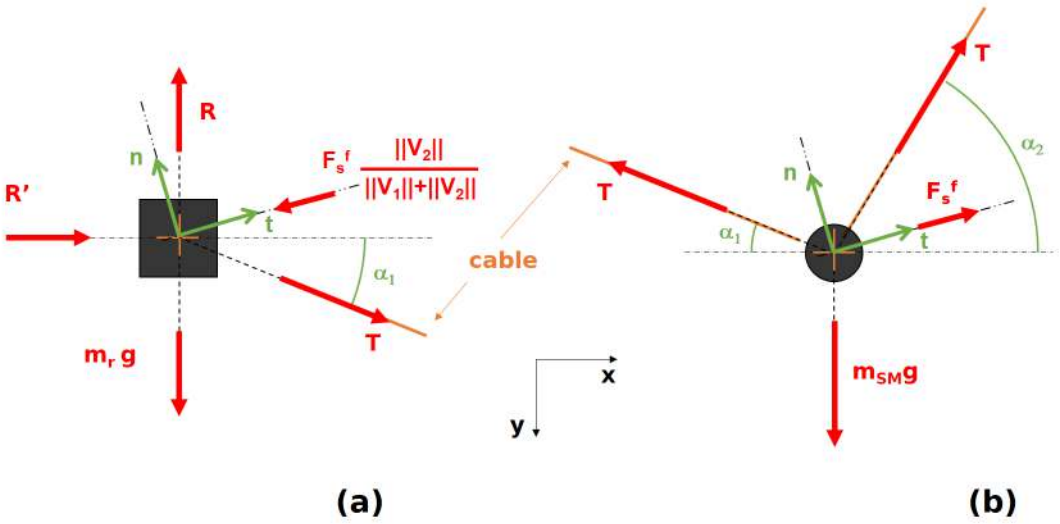

Figure 6: Mechanical force balance onto the mass-spring system (a) and onto the sliding mass (b).

$l_1^{ini} = \sqrt{(x^{ini} - x_r^{ini})^2 + (y^{ini})^2}$ and $l_2^{ini} = \sqrt{(2d - x^{ini})^2 + (y^{ini})^2}$ where ^{ini} refers to the initial values of each variables.

The mechanical balance of the mass connected to the spring is described in figure 6a and leads to the following equations

$$T\cos\alpha_1 + R' - \frac{\|\vec{V_2}\|}{\|\vec{V_1}\| + \|\vec{V_2}\|}\vec{F_s^f}.\vec{x} = m_r\,\ddot{x_r} \tag{26}$$

$$m_r\,g + T\sin\alpha_1 - R - \frac{\|\vec{V_2}\|}{\|\vec{V_1}\| + \|\vec{V_2}\|}\vec{F_s^f}.\vec{y} = m_r\,\ddot{y_r} \tag{27}$$

where $R' = -k_r\,x_r$. In order to be solved , the previous differential system can be expressed as

$$\begin{cases} \ddot{x} = \frac{1}{m_{\mathbf{SM}}}\Big(k_c(\Delta l_1 + \Delta l_2)(\cos\alpha_2 - \cos\alpha_1) + \vec{F}_s^f.\vec{x}\Big) \\ \ddot{y} = \frac{1}{m_{\mathbf{SM}}}\Big(m_{\mathbf{SM}}\, g - k_c(\Delta l_1 + \Delta l_2)(\sin\alpha_1 + \sin\alpha_2) + \vec{F}_s^f.\vec{y}\Big) \\ \ddot{x_r} = \frac{1}{m_r}\Big(k_c(\Delta l_1 + \Delta l_2)\cos\alpha_1 - k_r\, x_r - \dfrac{\|\vec{V_2}\|}{\|\vec{V_1}\| + \|\vec{V_2}\|}\vec{F}_s^f.\vec{x}\Big) \end{cases} \tag{28}$$

where the second member of the previous system only depends on the kinematic unknowns X and $\dot{X}$ where $X = [x,\, y,\, x_r]$.

3.2 Comparison between finite elements and RK4 solutions

Thus, the unknown displacements (x, y and x_r) are obtained through time by solving the equation of motion. The latter can be either solved by `RK4` approach or using finite element method. The results obtained by `RK4` method serve as reference and the solution coming from the finite element are compared to `RK4` solution. Within the framework of the finite element method, the validation model is simulated using the proposed macro finite element connected to a truss finite element. Only two finite elements are part of the finite element mesh. The initial mesh of the FE model in presented in figure 5b. The cable and the sliding mass kinematics are described within the macro finite element. The truss element, so-called the mass-spring **MS** system, simulates the elastic spring stiffness (k_r) and the concentrated mass (m_r). The integration scheme is explicit and the critical timestep is computed as

$$dt_c < \min\{dt_c^{Cable},\, dt_c^{\mathbf{SM}},\, dt^{\mathbf{MS}}\} \tag{29}$$

where $dt_c^{Cable} = \frac{1}{10}2\pi\sqrt{m_i/k_i}$ (resp. $dt_c^{\mathbf{SM}} = \frac{1}{10}2\pi\sqrt{m_{\mathbf{SM}}/k_i}$ and $dt_c^{\mathbf{MS}} = \frac{1}{10}2\pi\sqrt{m_r/k_r}$) is related to the cable (resp. the sliding mass and the mass-spring system). $k_i = E_c A_c/l_{ini}$ is the cable element stiffness of the i^{ieme} cable element. The timestep is chosen as $dt < dt_c$.

3.2.1 [ZAL04]'s case study

In the case presented in [ZAL04], an inextensible cable is used and no mass-spring system is considered (fixed cable ends). The sliding mass interacts

Inputs	**Description**	**Value**	**Units**
Gravity	g	3.05	m/s^2
Geometry	d	0.3	m
Init. Position **SM**	x_ini	0.15	m
Init. Position **SM**	y_ini	0.15	m
Init. Velocity **SM**	xpt_ini	0	m/s
Init. Velocity **SM**	ypt_ini	0	m/s
Init. Position **MS**	xr_ini	0	m
Init. Velocity **MS**	xrpt_ini	0	m/s
MS mass	m_r	15×10^8	kg
SM mass	$m_{\mathbf{SM}}$	100	kg
MS Stiffness	k_r	10^8	N/m
Cable Stiffness	k_c	4.58×10^8	N/m
Cable *Young*'s Modulus	E_c	1000×10^9	Pa
Cable cross-section	A_c	3.14×10^{-4}	m^2
Cable radius	r_c	0.01	m
Init. Cable length	$L_c^{ini} = l_1^{ini} + l_2^{ini}$	0.6865	m
Friction	μ	0	(-)
Timestep	$dt = \frac{T_{max}}{Ntps}$	1.25×10^{-4} (6.6×10^{-5})	s

Table 1: Inputs of [ZAL04]'s study case (inextensible cable, no friction and fixed cable ends). Black (resp. blue) values are related to RK4 (resp. FE) approach. **SM** for sliding mass and **MS** for mass-spring.

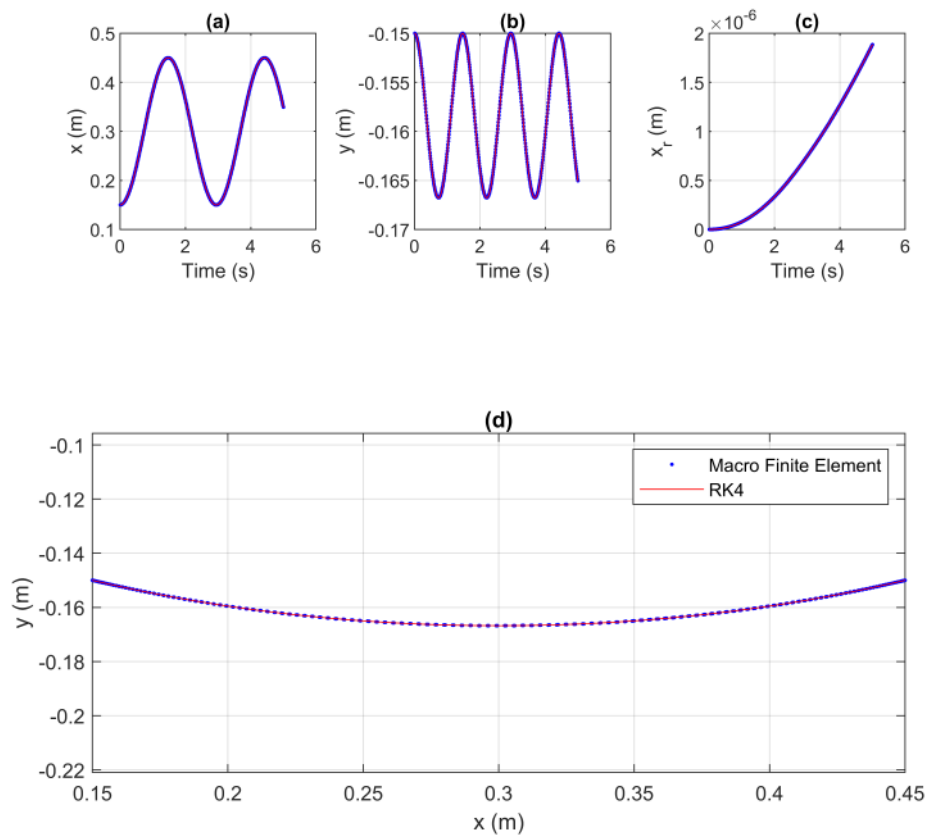

Figure 7: Case of [ZAL04] (inextensible cable, no friction, fixed cable ends). Comparison between FE model and the RK4 displacements.

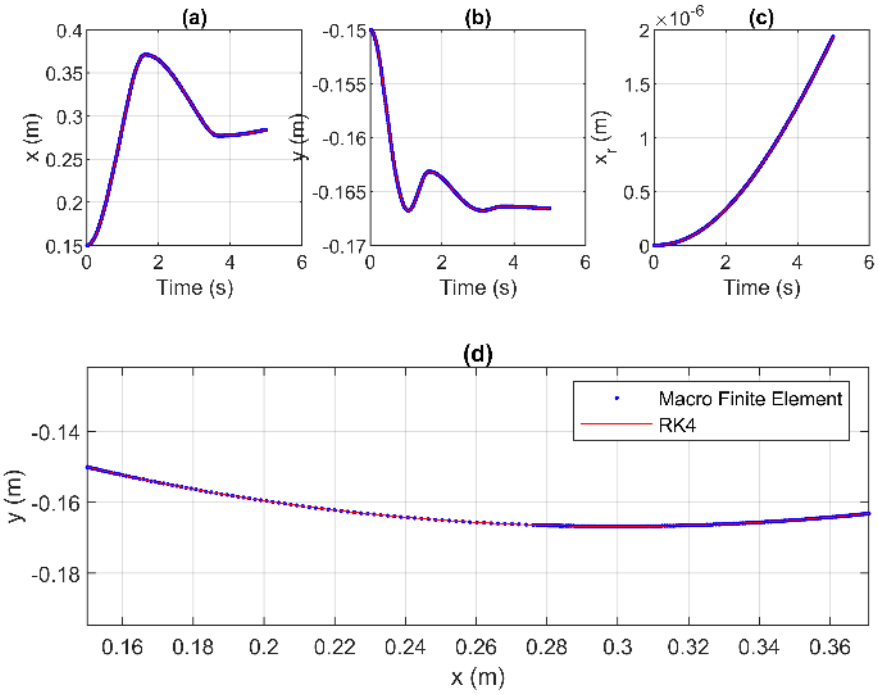

Figure 8: Case of [ZAL04] (inextensible cable, with a friction coefficient of 0.1, fixed cable ends). Comparison between FE model and the RK4 displacements.

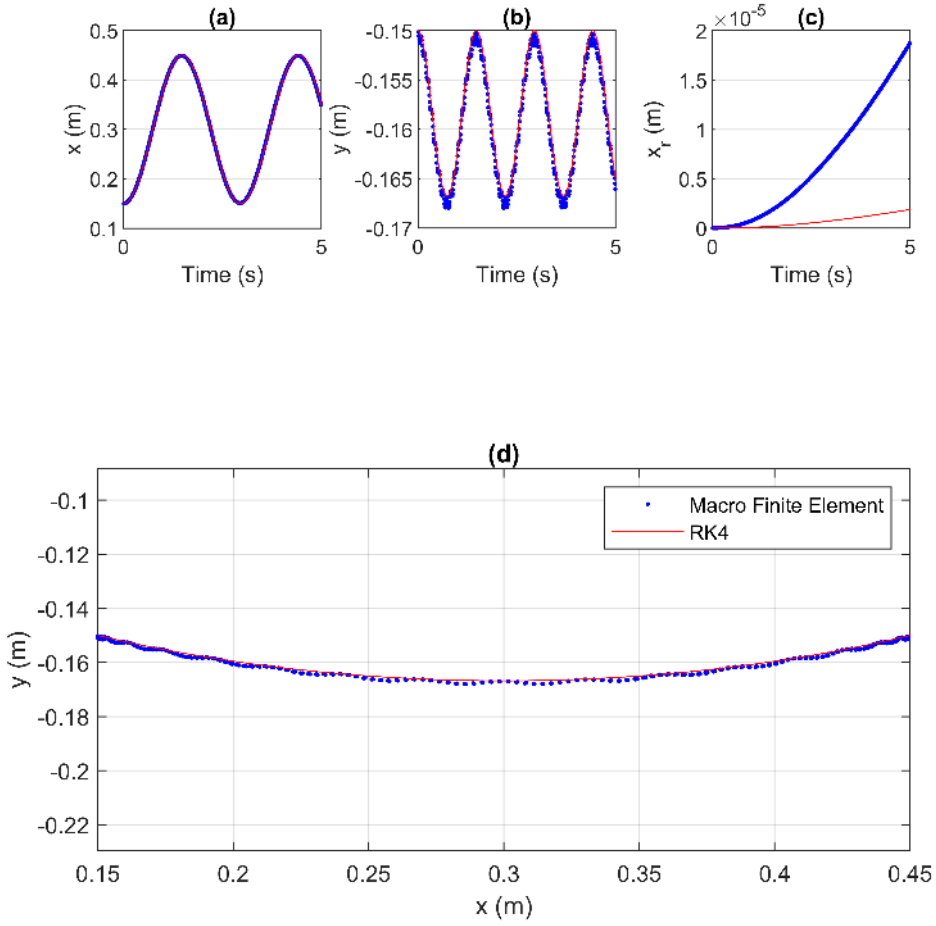

Figure 9: Case of [ZAL04] (inextensible cable, no friction, fixed cable ends) in the case of a discretized cable (8 segments in the DEM model) within the macro finite element. Comparison between FE model and the RK4 displacements.

Inputs	Description	Value	Units
MS mass	m_r	1500	kg
SM mass	$m_{\mathbf{SM}}$	1000	kg
MS Stiffness	k_r	10^5	N/m
Cable Stiffness	k_c	4.58e^6	N/m
Cable *Young*'s Modulus	E_c	10e10^9	Pa

Table 2: Inputs of the RK4 approach (in black) and of the macro finite element when considering the effect of the **MS** system.

with the cable without friction. A very high cable longitudinal stiffness and a very high mass for the mass-spring system have been considered in order to fit with the inextensible conditions of the cable and the cable boundary conditions. In order to be as close as possible of the conditions of [ZAL04], a single cable element has been considered for the discretization of the cable. The table 1 summarizes the inputs used for the case proposed in the paper of [ZAL04].

In the figure 7, a perfect agreement is shown, on the one hand between both resolutions process (FE and RK4 methods), and on the other hand results are in complete adequacy with the solution presented by [ZAL04].

The effect of friction has been explored. A friction coefficient of 0.1 has been considered and the same simulation has been performed. Figure 8 shows a very good agreement between the results coming form the FE model and the RK4 resolution.

Finally, the effect of the cable discretization has been underlined (Figure 9). The cable density has been set at $\rho_c = 8000$ kg/m^3 and the cable has been meshed with 8 cable elements (8 segments in the DEM model). The solution of the FE model is very close to the RK4 solution. The small observed variations are related to the mass of the cable which is not accounted for in the case of [ZAL04] thus within the RK4 formulation of the problem.

3.2.2 Cross validation: FE and RK4 resolutions

The effect of the **MS** system is now investigated. The validation of the macro element implementation is performed by considering the potential displacement of the mass m_r. The table 2 summarizes the inputs which have been changed from the [ZAL04]'s case. The parameters are chosen such as to allow the development of significant displacements of the **MS** system.

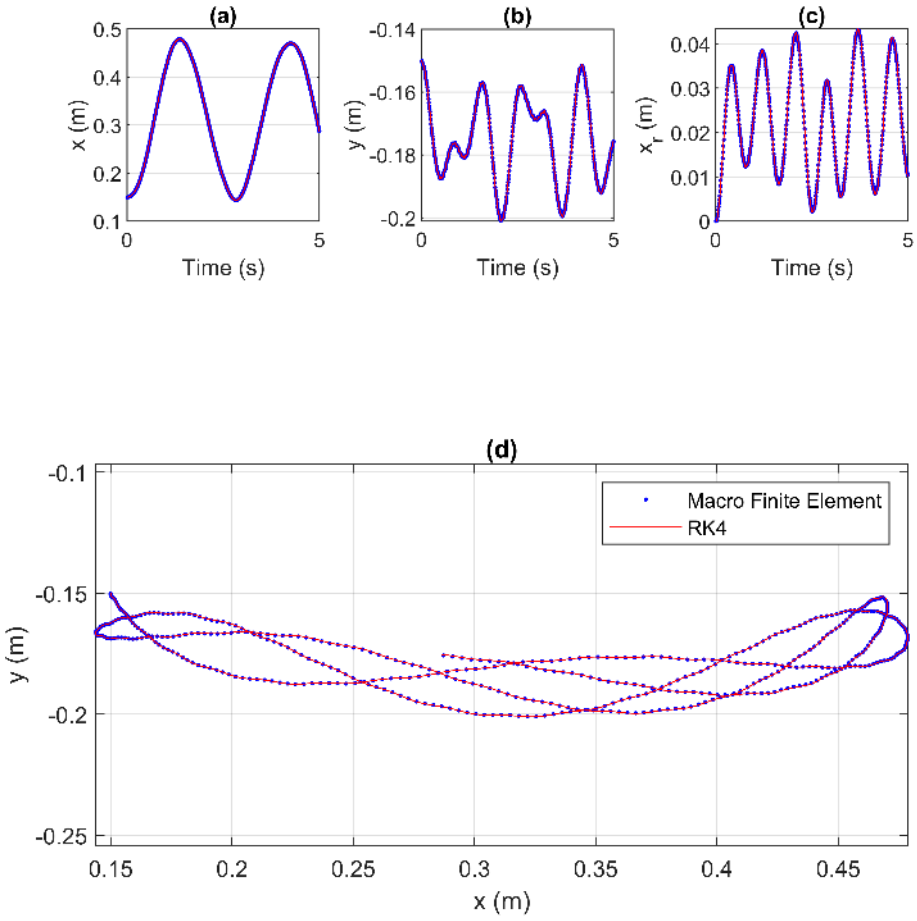

Figure 10: **MS** system effect in the case of no friction and a single cable element used to mesh the cable. Comparison between FE model and the RK4 displacements.

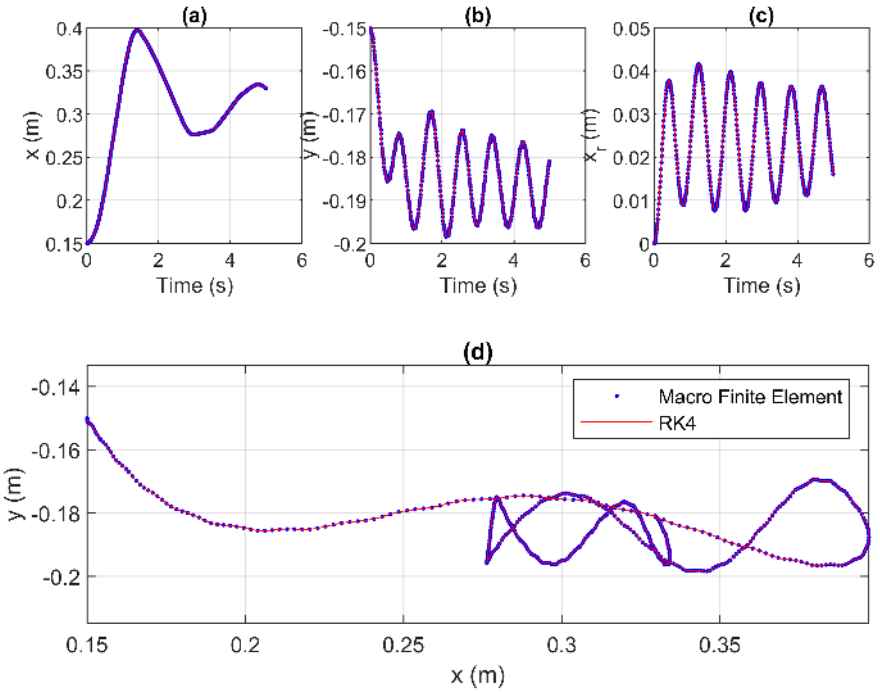

Figure 11: **MS** system effect in the case of a friction coefficient of 0.1 and a single cable element used to mesh the cable. Comparison between FE model and the RK4 displacements.

First, two simulations (with and without friction) have been preformed considering a single cable element (Figures 10 and 11). In both cases (friction and no friction), a very good agreement is observed even if the trajectory of the slider is in some extent rather complex.

Then, the same simulations have been carried out using 8 cable elements to discretize the cable considering a mass density of $\rho_c = 8000$ kg/m^3. Once again, without friction, a very good agreement is observed (Figure 12). If friction is considered a significant discrepancy can be noticed (Figure 13). It can be explained by the wave propagation that can now occur within the cable. The discretization of the cable enables waves to propagate along the longitudinal axis which is not the case when only one cable element is accounted for. The RK4 solution cannot serve as a reference solution because the validation model is not able to describe such physics.

4 Applications examples

4.1 Cable yarning

As an illustration of the capabilities of the proposed macro finite element, an application to cable yarning is proposed. The interaction between usual finite elements and a macro finite element is illustrated in figure 14a. In this application, an elastic cable is placed between two flexible posts having a length $H_b = 5$ m (Figure 14a). The two posts are separated by a horizontal (resp. vertical) distance $X_b = 20$ m (resp. $Y_b = 4$ m). A sliding object can move onto the cable under the action of gravity. The posts are modelled with usual *Timoshenko* beam finite elements. The finite element mesh is depicted in figure 14b. The *Young*'s modulus of the posts is $E_b = 200$ GPa (steel) and its density equals $\rho_s = 8000$ kg/m^3. The cross section is supposed rectangular with a width of $b = 15$ cm and a depth of $h = 15$ cm. Thus, the second moment of area along z axis equals $I_b = bh^3/12 = 4218.7$ cm^4 which corresponds to a bending stiffness of $E_b I_b = 8.44$ MN.m^2. Each post is fixed at the bottom end and is composed of four finite elements having a length of 1.25 m.

The cable and the sliding mass are modelled with the proposed macro finite element where eight cable elements are used to mesh the cable and the sliding object has a mass of $m_{\mathbf{SM}} = 1000$ kg. At rest, the length of the cable is $L_c^{ini} = 1.0025 \times L_{post} = 20.45$ m where L_{post} (20.4 m) is the distance

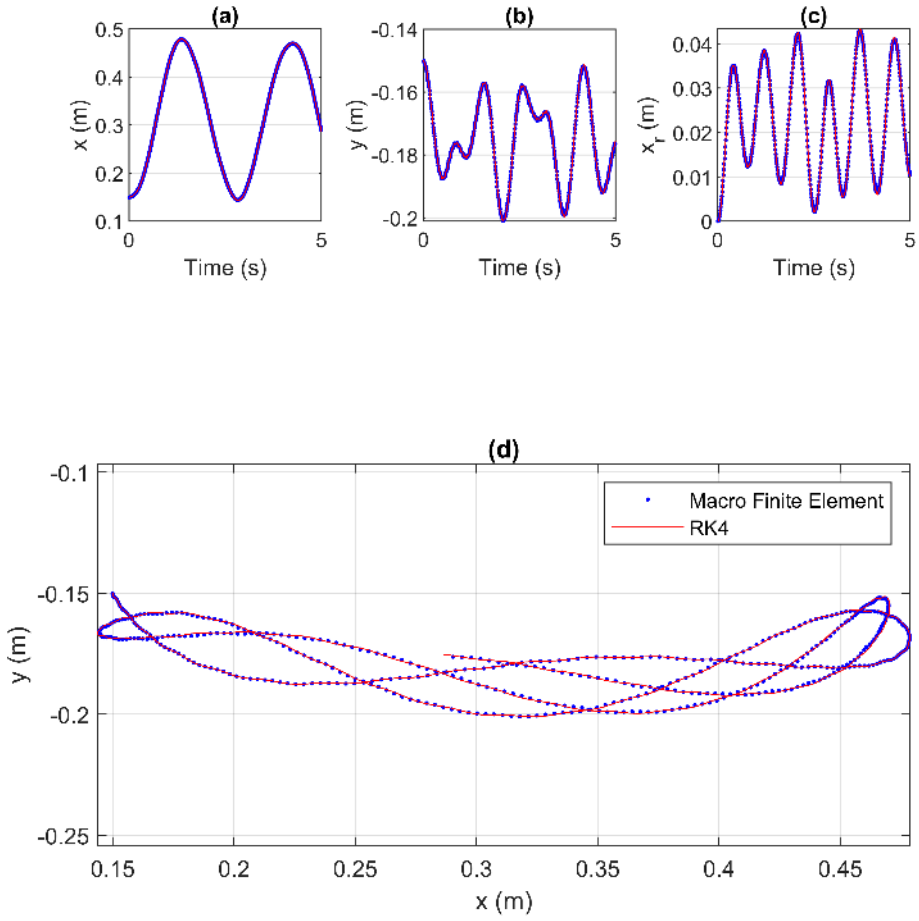

Figure 12: **MS** system effect in the case of no friction and 8 cable elements used to mesh the cable. Comparison between FE model and the RK4 displacements.

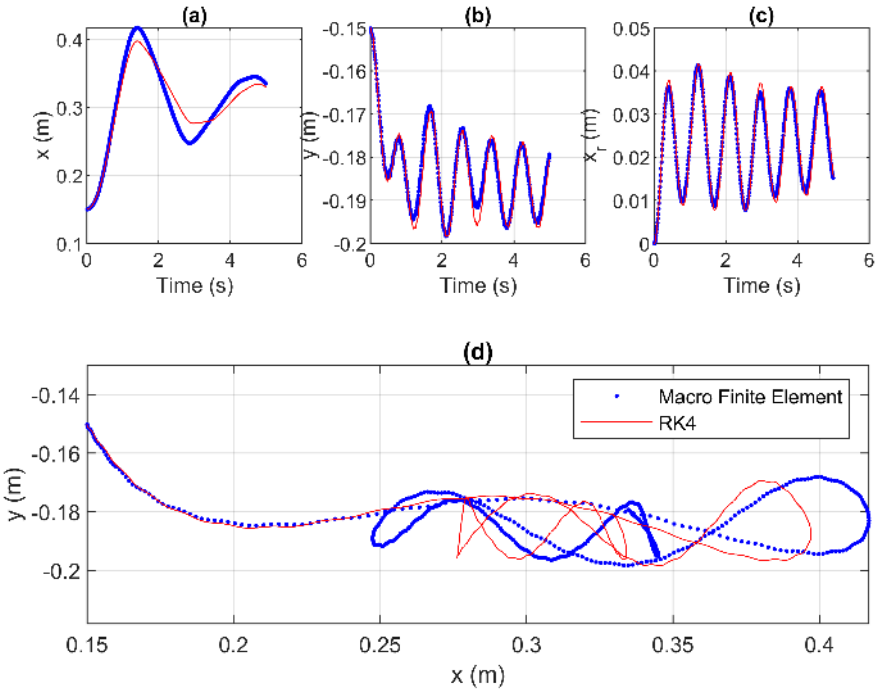

Figure 13: **MS** system effect in the case of a friction coefficient of 0.1 and 8 cable elements used to mesh the cable. Comparison between FE model and the RK4 displacements.

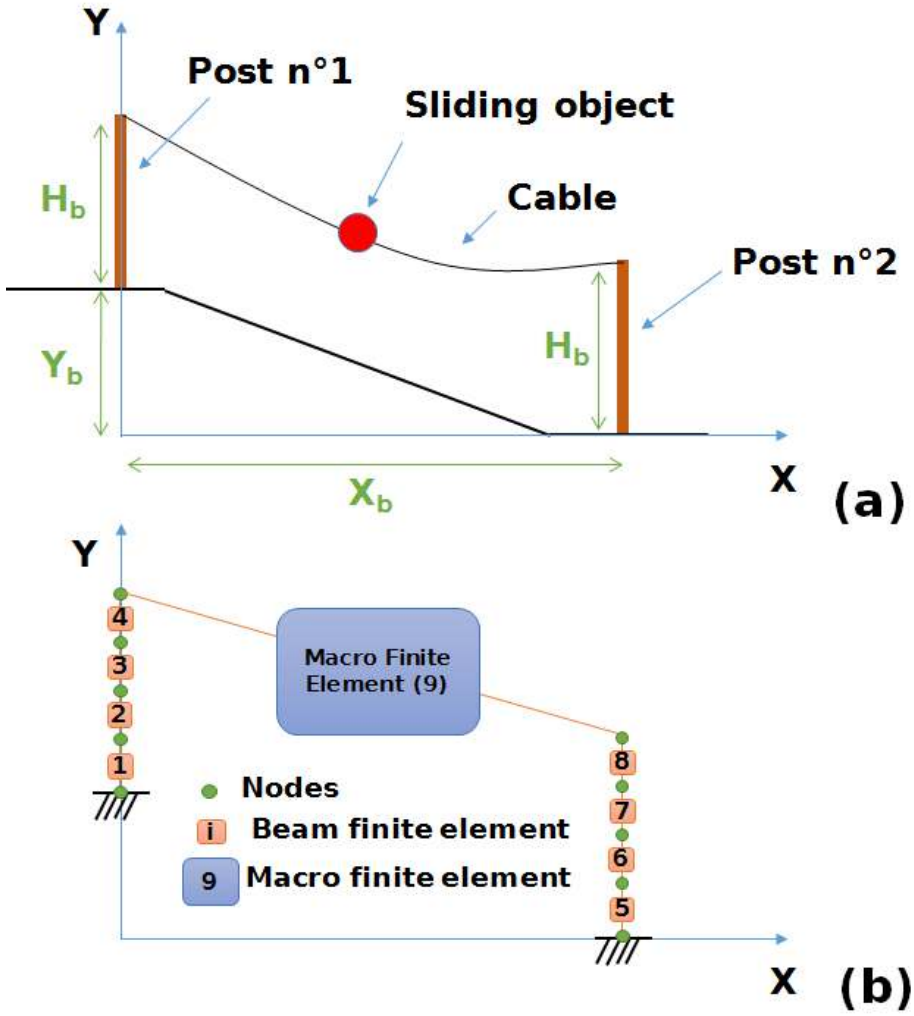

Figure 14: Application to cable yarning. A cable where a sliding mass can move under the action of gravity linking two elastic posts (a). Finite element mesh mixing usual finite elements (for instance *Timoshenko* beam) and a macro finite element (b).

between the post heads (top of the post), the diameter of the cable is d_c = 2 cm and its apparent *Young*'s modulus is supposed to be equal to $E_c = 5$ GPa and its density $\rho_c = 8000$ kg/m^3.

For a sake of simplicity, the cable is initially placed on a straight line between the two post heads (from (0,$Y_b + H_b$) to (X_b,H_b)). Then the sliding object is placed on the cable at 15% of the distance L_{post} along the straight line from the head of the post n^{o}1 (upstream post). Before the release of the sliding object, the initial static mechanical balance of the cable and of the sliding object have to be obtained under gravity. During that preliminary phase, the horizontal displacement of the sliding object is fixed and thus it can move only along y axis. A damping, based on acceleration reduction ([CS79]), is used to dissipate the kinetic energy allowing to reach a static equilibrium (sliding mass velocity lower than 0.001 m/s) in 4.5 s (simulated time). During this preliminary phase, the damping is chosen equal to 0.75 and then set to 0 for the second phase (dynamic phase). At $t = 4.5$ s, the sliding object is released which allows the motion of the sliding object along the cable. For each simulation, the total physical time simulated is 9 s. The effects of the post bending stiffness (E_bI_b) and the friction coefficient (μ) between the cable and the sliding object are investigated.

4.1.1 Influence of post stiffness

The bending stiffness varies through the second moment of area of the beam. b is kept constant (15 cm) and h equals respectively to (7.5, 10, 12.5, 15, 17.5) cm which corresponds to E_bI_b = (1.5, 2.5, 4.88, 8.44, 13.4) MN.m^2. An additional case considers the post as rigid solids (*quasi* infinite bending stiffness - 2500 MN.m^2). The friction is taken into account and the friction coefficient equals $\mu = 0.1$. Figure 15 depicts the results. The post bending stiffness has an influence on the kinematics of the sliding mass (Figure 15a). The maximal deflections can vary of more than 2 m and the slider trajectory is significantly modified. Similar observations can be performed for the velocity (Figure 15b) in particular for the vertical component which increases when the posts have a low bending stiffness.

The flexibility of the post allows reducing the forces within the cable. When the inclination angle of the cable with respect to the horizontal increases, the cable tension changes. The higher is the angle, the lower is the cable tension. Indeed, the slider generates mainly a vertical force into the cable and if the cable is horizontal, the cable tension becomes infinite. Thus,

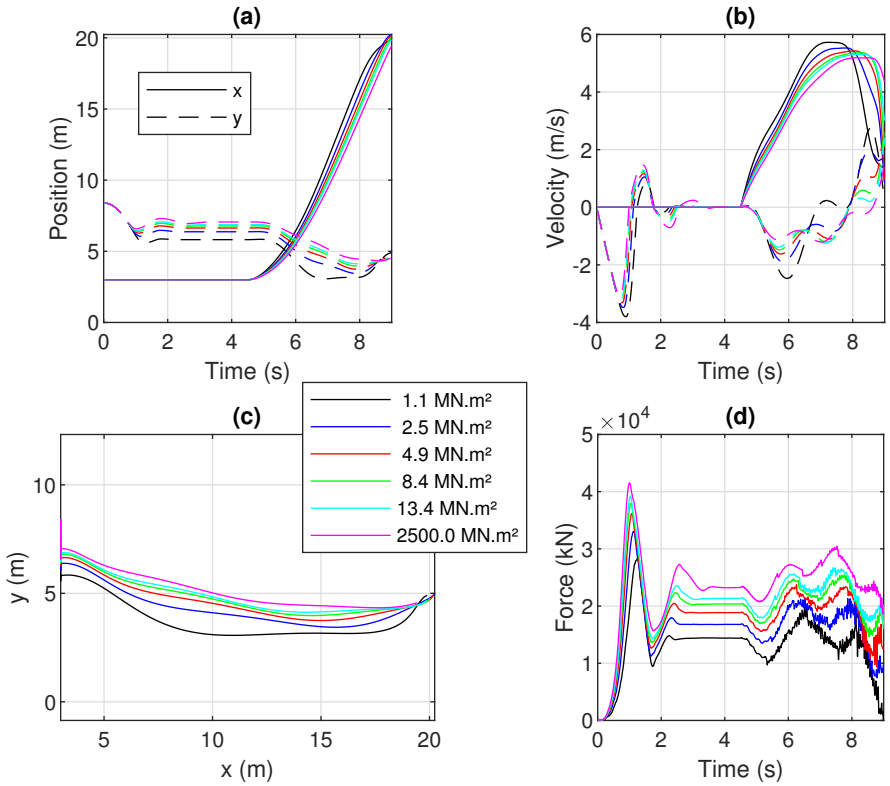

Figure 15: Effect of post stiffness (E_bI_b). Time evolution of the sliding mass position (resp. velocity) (a) (resp. (b)), sliding mass trajectory (c) and time evolution of the cable tension (d).

the cable tension is higher for a case of rigid posts (Figure 15d). Moreover, cable tension oscillations increase when the post flexibility is high due to the development of vertical oscillations of the slider which are amplified by the post elastic response.

4.1.2 Influence of friction

The friction coefficient equals respectively (μ = 0, 0.1, 0.2, 0.3) and the bending stiffness E_bI_b =8.44 MN.m^2. The friction coefficient has a much more significant effect on the results (Figure 16) than the bending stiffness. First, the kinematics of the sliding object is much more influenced (Figure 16a-c). The more the friction increases, the more the movement is reduced.

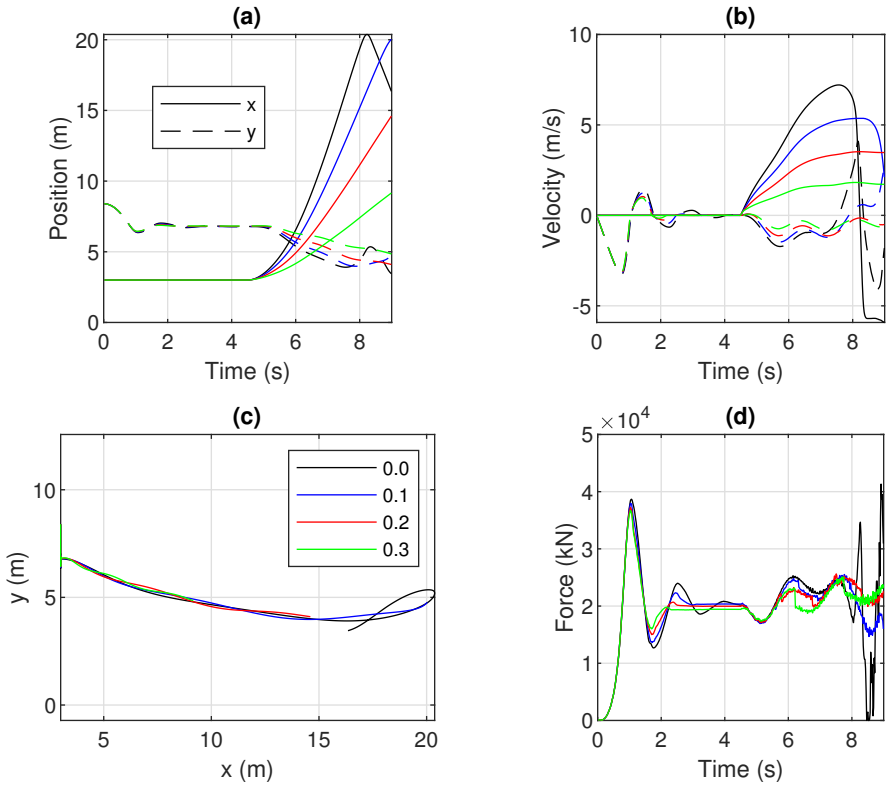

Figure 16: Effect of the friction coefficient (μ). Time evolution of the sliding mass position (resp. velocity) (a) (resp. (b)), sliding mass trajectory (c) and time evolution of the cable tension (d).

The kinematics is also strongly impacted (Figure 16b). The velocity of the sliding mass is significantly reduced when friction interaction between the slider and the cable is accounted for. Finally, the oscillations over time of the force applied to the post head (Figure 16d) are rather reduced when the friction coefficient increases.

4.2 Cable-stayed bridge

Another example focuses on the modelling of cable-stayed bridges. This example illustrates how to model under the same computational environment, several flexible cables and rigid beams. Here, no sliding object is taken into

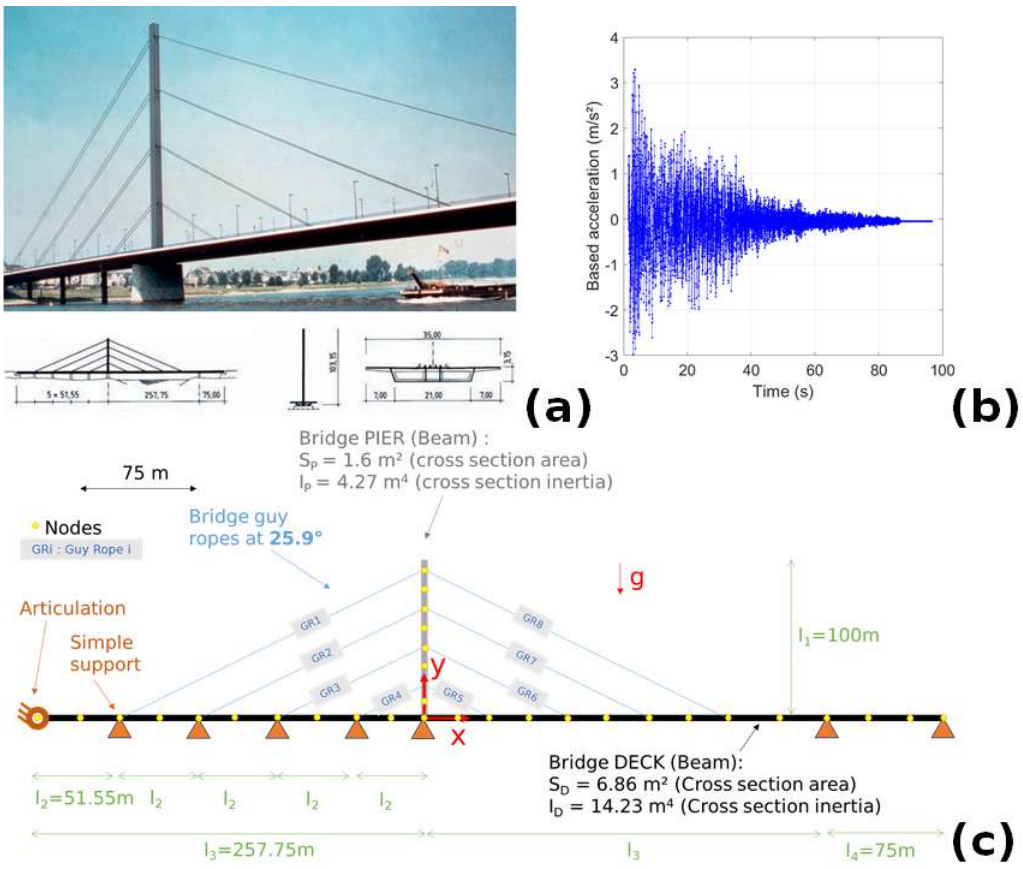

Figure 17: Steel cable-stayed Bridge of Oberkassel in Germany inaugurated in 1976 ([Sve12] (a). Seismic input applied to the structure based on the EC8 response-spectra shape (b). Simplified cable-stayed bridge finite element model (c). Geometry, main components, boundary conditions, and related meshing mixing beam finite elements and macro finite elements (Guy Ropes).

account onto the cables but cables can still describe large displacements. It underlines the flexibility of the use of such macro finite elements. A rather simple idealized bridge is considered and is inspired from the Oberkassel Bridge (Germany) which has been inaugurated in 1976 ([Sve12]). As the objective of this paper is not to assess the behaviour of this bridge, the geometrical and material parameters are chosen as realistically as possible, but are not the actual values. It is composed of a single pier and a deck made of steel (Figure 17a). The cables are in harp arrangement.

From a numerical point of view, its geometry and the meshing are presented in Figure 17c. For the sake of simplicity, the model is proposed in two dimensions but can be easily generalized to 3D problems. A pier (100 meters high) is connected to the deck by 8 guy ropes modelled as macro finite elements. The number of cable elements for each guy rope is from GR1 to GR8 respectively [12 10 7 5 5 7 10 12]. The damping of the cable nodes is set to zero. The diameter of the cable is $D_c = 400$ mm, the equivalent *Young*'s modulus is $E_c = 5$ GPa and its density is supposed to be equal to 4660 kg/m^3 assuming that the linear mass of the cable having a diameter of 40 mm equals 5.85 kg/m, so for a cable of 400 mm its linear density is 585.6 kg/m.

The cross-section area and second moment of area have been assessed from [Sve12]. The pier (resp. the deck) is supposed to have a cross-section area of $S_P = 1.6$ m^2 (resp. $S_D = 6.86$ m^2) and a second moment of area of $I_P = 4.27$ m^4 (resp. $I_D = 14.23$ m^4). The deck and the pier are supposed made of steel (*Young*'s modulus $E_b = 200$ GPa and density 7500 kg/m^3). The bridge is subjected to an earthquake characterized by a seismic input presented in Figure 17b. Each guy rope is prestressed (100 kN).

The effect of a cable failure during the earthquake is investigated. Four cases are considered (Figure 18)). The first one is the response of the structure without applying an earthquake which can serve as a reference. The next case gives the response of the bridge under the earthquake considering no guy rope failure occurrence. The third (resp. the fourth) case simulates the failure of the guy rope 8 (resp. 8 and 4) at time equals 7.35 s (resp. 7.35 s and 7.65 s) when the peak ground acceleration has just been reached.

Figures 19a-b (cases without guy rope failure) and 19c-d (cases with guy rope failure) depict the time evolution along the pier axis of the displacement field and the internal efforts (Axial force, shear force and bending moment) within the pier. It can be noted that the earthquake excitation does not have significant effect on the response of the bridge when no guy rope fails.

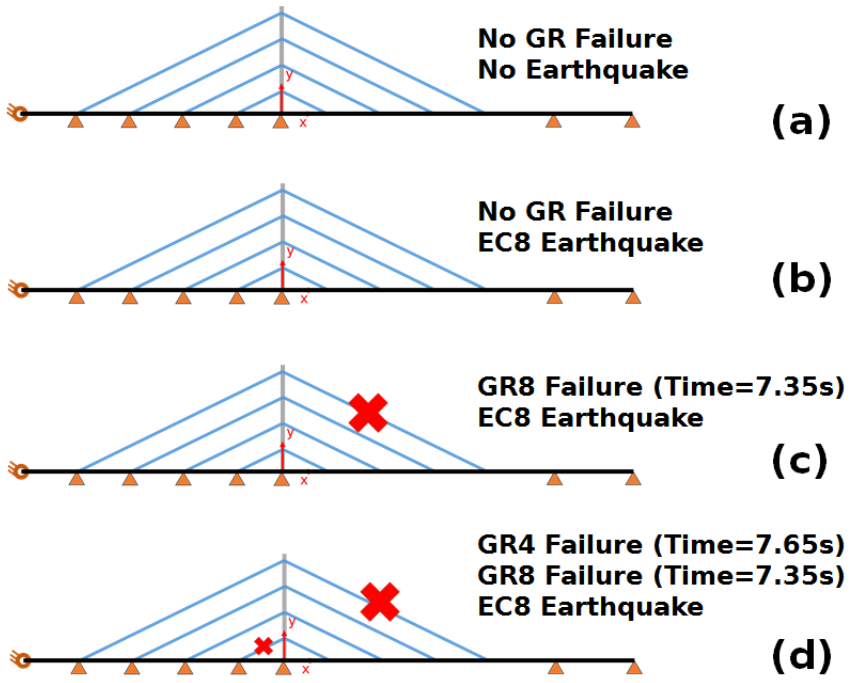

Figure 18: Guy rope failure senarii. No guy rope failure (a and b) and with guy rope failure occurrence (c and d).

The maximal displacement stays small compared to the reference case and the same remark can be made for the internal efforts. When one or two guy rope failures occur, the pier exhibits a significant drop of axial force (due to the loss of prestress) and a notable increase of bending moment especially in the neighbourhood of the fixation point of the failed guy rope. For the same scenario with an additional guy rope failure (GR4), an increase of the base shear force can be noted.

Thus, these simple simulations can give very interesting insights concerning the response of cable based bridges under a large amount of failure scenarii (earthquake, impact, wind, *etc.*) and using very ergonomic, robust numerical tools.

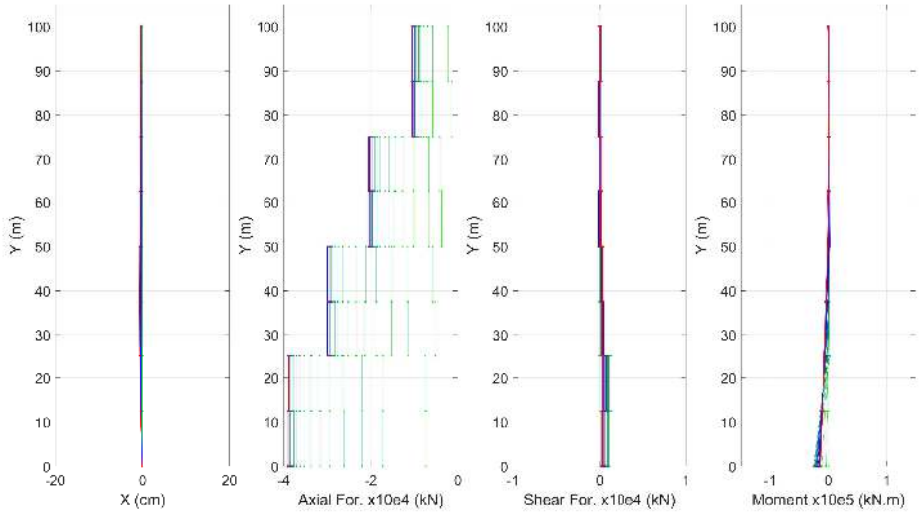

(a) No GR Failure - No earthquake

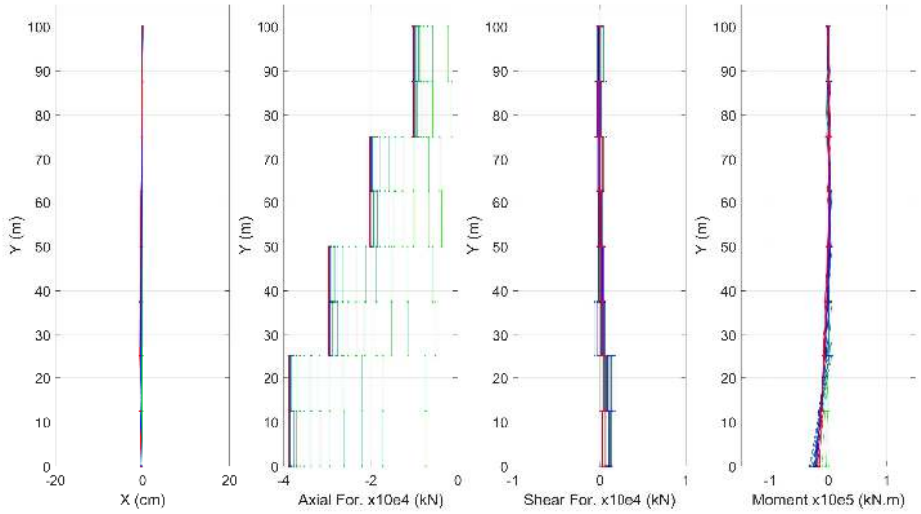

(b) No GR Failure - EC8 earthquake

Figure 19: No guy rope failure senarii. Time evolution along the pier of the horizontal displacements, the axial and shear forces and the bending moment. The time evolution is depicted by the following colour code : from green ($t = 0$ s) to red (t =end of simulation). The following cases are shown for the pier response : under its own weight and without guy rope failure (a) and under EC8 earthquake without guy rope failure (b).

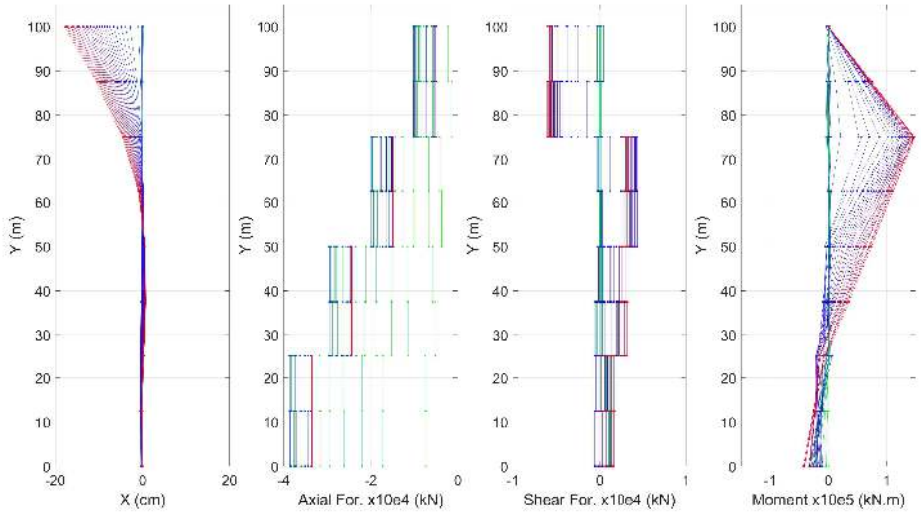

(c) GR8 Failure (Time = 7.35 s) - EC8 earthquake

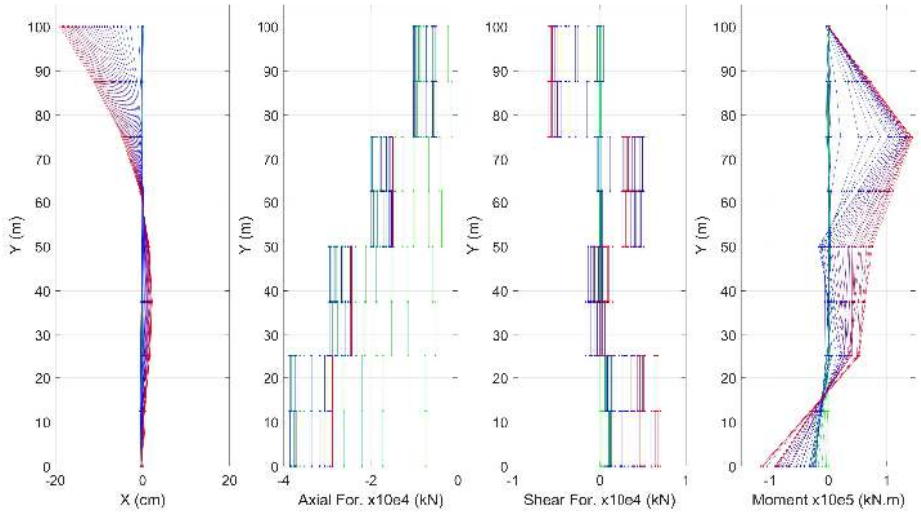

(d) GR4 (Time = 7.65 s) and GR8 (Time = 7.35 s) Failure - EC8 earthquake

Figure 20: Guy rope failure senarii. Time evolution along the pier of the horizontal displacements, the axial and shear forces and the bending moment. The time evolution is depicted by the following colour code : from green ($t = 0$ s) to red (t =end of simulation). The following cases are shown for the pier response : Under EC8 earthquake with the failure of GR8 (c) and under EC8 earthquake with the failure of GR4 and GR8 (d).

5 Conclusion

A novel approach for modelling cable based structures was presented. The resolution of the problem has been performed within a dynamic framework using the concept of *macro finite element* in order to couple FEM and DEM approaches. It allows modelling under the same computational environment several types of structures which can have very different mechanical behaviours. In addition, DEM is particularly well suited to model cable systems without extensive mathematics development as within a fully finite element framework. A specific macro finite element which contents all the cable physics (behaviour law, large displacement/strains, interaction with sliding object, *etc.*) has been formulated and implemented within an usual finite element procedure. This approach is particularly interesting because of its simplicity to implement such DEM modelling within classical finite element codes. Multiple comparison examples demonstrated that the FEM-DEM coupling is validated. Finally, as an illustration of the capabilities of the approach, a parametric study has been performed to underline the effect of the coupling of rigid and flexible structures.

Because of the flexibility of the macro finite element formulation, its adaptation to a specific case can be done without major difficulty. For instance, if it is needed to connect the sliding mass to another finite element node of the mesh (to model pulley connection), the inputs and outputs should be adapted leading to consider three nodes instead of two (as presented into the paper).

For the moment, the numerical integration scheme should be the same at the scale of the macro finite element and at the global scale (finite element code scale), thus if the macro finite element is formulated with the help of the DEM, the calculation must use central finite different integration scheme at both scale. In terms of perspectives, in order to reduce the computational cost, several types of integration schemes can be mixed with HATI (Heterogeneous and Asynchronous Time Integrations) approaches based one primal coupling technics. Indeed, the macro finite element can be considered as a sub-domain.

References

[AAG95] H. Ali and A. Abdel-Ghaffar. Modeling the nonlinear seismic behavior of cable-stayed bridges with passive control bearings. *Computers and Structures*, 54(3):461–492, 1995.

[Alb16] A. Albaba. *Discrete element modeling of the impact of granular debris ows on rigid and exible structures*. PhD thesis, Université Grenoble Alpes, 2016.

[AQNO03] M. Al-Qassab, S. Nair, and J. O'Leary. Dynamics of an elastic cable carrying a moving mass particle. *Nonlinear Dynamics*, 33(1):11–32, 2003.

[Auf93] M. Aufaure. A finite element of cable passing through a pulley. *Computers and Structures*, 46(5):807 – 812, 1993.

[BB04] W. Bin-Bing. *Free-Standing Tension Structures - From tensegrity systems to cable-strut systems*. Spon Press, 2004.

[BTLS12] D. Bertrand, A. Trad, A. Limam, and C. Silvani. Full-scale dynamic analysis of an innovative rockfall fence under impact using the discrete element method: from the local scale to the structure scale. *Rock Mechanics and Rock Engineering*, 45(5):885–900, 2012.

[CCLN17] J. Coulibaly, M. Chanut, S. Lambert, and F. Nicot. Sliding cable modeling: An attempt at a unified formulation. *International Journal of Solids and Structures*, 2017.

[CG02] A. Combescure and A. Gravouil. A numerical scheme to couple subdomains with different time-steps for predominantly linear transient analysis. *Comput. Methods Appl. Mech. Engrg.*, 191:1129–1152, 2002.

[CS79] P.A. Cundall and O.D.L. Strack. A discrete numerical model for granular assemblies. *Géotechnique*, 29 (1):47–65, 1979.

[DBB16] S. Dupire, F. Bourrier, and F. Berger. Cablehelp: a model for predicting load path and tensile forces during 1 cable yarding

operations in mountain forests. *Journal of Forest Research*, 21(1):1–14, 2016.

[DBYK11] S. Dhakal, N. Bhandary, R. Yatabe, and N. Kinoshita. Experimental, numerical and analytical modelling of a newly developed rockfall protective cable-net structure. *Nat. Hazards Earth Syst. Sci.*, 11:3197–3212, 2011.

[DCB+19] L. Dugelas, J. Coulibaly, F. Bourrier, S. Lambert, M. Chanut, I. Olmedo, and F. Nicot. Assessment of the predictive capabilities of discrete element models for flexible rockfall barriers. *International Journal of Impact Engineering*, 133:1–6, 2019.

[DV99] T.P. Dreyer and J.H. VanVuuren. A comparison between continuous and discrete modelling of cables with bending stiffness. *Applied Mathematical Modelling*, 23(7):527 – 541, 1999.

[FS11] F. Ferreira and L. Simoes. Optimum design of a controlled cable stayed bridge subject to earthquakes. *Struct Multidisc Optim*, 44:517–528, 2011.

[GGM+12] C. Gentilini, L. Govoni, S. Miranda, G. Gottardi, and F. Ubertini. Three-dimensional numerical modelling of falling rock protection barriers. *Computers and Geotechnics*, 44:58–72, 2012.

[Irv81] H.M. Irvine. *Cable structures*. MIT Press, Cambridge, MA, 1981.

[JC05] F. Ju and Y.S. Choo. Super element approach to cable passing through multiple pulleys. *International Journal of Solids and Structures*, 42(11–12):3533 – 3547, 2005.

[LCJ03] K. Lee, Y. Choo, and F. Ju. Finite element modelling of frictional slip in heavy lift sling systems. *Computers and Structures*, 81:2673–2690, 2003.

[MGB+16] A. Mentani, A. Giacomini, O. Buzzi, L. Govoni, G. Gottardi, , and S. Fityus. Numerical modelling of a low-energy rockfall barrier: New insight into the bullet effect. *Rock Mech Rock Eng*, 49:1247–1262, 2016.

[NCM01] F. Nicot, B. Cambou, and G. Mazzoleni. Design of rockfall restraining nets from a discrete element modelling. *Rock Mechanics and Rock Engineering*, 34 (2):99–118, 2001.

[Sve12] H. Svensson. *Cable-Stayed bridges - 40 Years of Experience Worldwide*. Ernst and Sohn, 2012.

[TIWYM94] Tadibakhsh, G. Iradi, Wang, and Yi-Ming. Transient vibrations of a tau inclined cable with a riding accelerating mass. *Nonlinear Dynamics*, 6(2):143–161, 1994.

[TK11] H. Thai and S. Kim. Non linear static and dynamic analysis of cable structures. *Finite Elements in Analysis and Design*, 47:237–246, 2011.

[WC89] J-S. Wu and C-C. Chen. The dynamic analysis of a suspended cable due to a moving load. *International Journal for Numerical Methods in Engineering*, 28(10):2361–2381, 1989.

[Wil06] P. Williams. Dynamics of a cable with an attached sliding mass. In Andrew Stacey, Bill Blyth, John Shepherd, and A. J. Roberts, editors, *Proceedings of the 7th Biennial Engineering Mathematics and Applications Conference, EMAC-2005*, volume 47 of *ANZIAM J.*, pages C86–C100, July 2006. http://anziamj.austms.org.au/V47EMAC2005/Williams [July 7, 2006].

[ZAL04] B. Zhou, M.L. Accorsi, and J.W. Leonard. Finite element formulation for modeling sliding cable elements. *Computers and Structures*, 82(2–3):271 – 280, 2004.

[ZC14] Y. Zhou and S. Chen. Time-progressive dynamic assessment of abrupt cable-breakage events on cable-stayed bridges. *Journal of Bridge Engineering*, 19(2):159–171, 2014.